



Modelling Velocity Distribution in 3-D for Nun River, Niger Delta Nigeria

Desmond U. Nwoko¹, Ify L. Nwaogazie^{2*} and Charles C. Dike¹

¹Centre for Occupational Health Safety and Environment, University of Port Harcourt, Nigeria.

²Department of Civil and Environmental Engineering, University of Port Harcourt, Nigeria.

Authors' contributions

This work was carried out in collaboration between all authors. Author DUN carried out literature review survey, data collection and computer simulation. He wrote the protocol as well as the first draft of the manuscript. Author ILN served as main supervisor reviewed the research designed, computer method and documentation. Author CCD as assistant supervisor managed the computer simulation. All authors read and approved the final manuscript.

Article Information

DOI: 10.9734/BJAST/2017/33352

Editor(s):

(1) Vyacheslav O. Vakhnenko, Division of Geodynamics of Explosion, Subbotin Institute of Geophysics, National Academy of Sciences of Ukrainian, Ukraine.

Reviewers:

(1) Rajkumar V. Raikar, KLE Dr. M. S. Sheshgiri College of Engineering and Technology, Belagavi, India.

(2) Chiadikobi, Kingsley, Chukwuemeka Odumegwu Ojukwu University, Uli, Anambra State, Nigeria.

Complete Peer review History: <http://www.sciencedomain.org/review-history/18966>

Original Research Article

Received 11th April 2017
Accepted 30th April 2017
Published 8th May 2017

ABSTRACT

In this study, hydrodynamics and sediment concentration equations of partial differential in 3-dimensions were solved using finite difference methods, the Crank Nicolson procedure to predict both sediment concentration and velocity profile of Nun River. The computer software (EKU2.8) which is a modification of the Navier Stoke's equations was employed for discretization of Nun River stretch of 2,000 m into 2,245 rectangular meshes and simulation of the river's flow velocity distribution. The code was validated by using the field water current measurements obtained from a selected stretch of the river. Average predicted velocities of 0.85 m/s, 1.542 m/s and 0m/s compared favorably with 0.8m/s, 1.475 m/s and 0.09m/s obtained from field measurement for upstream, midstream and downstream boundaries. The predicted results have approximate correlation coefficients of 0.96 for velocity distribution using Pearson product-moment method. The model proved very useful in predicting the velocity distribution of Nun River; higher versus lower velocities at inner and outer bends, with resultant effect of erosion and sediment deposition accordingly. The result of this study may be considered an important contribution to the improvement of sediment and erosion risk management.

*Corresponding author: E-mail: ifynwaogazie@yahoo.com;

Keywords: Modelling; velocity; erosion; sediment; three dimensions; Nun River; Niger Delta.

1. INTRODUCTION

Rivers are constantly in motion by nature and they adjust their flow patterns with respect to any change in the river geometry or bathymetry. These environmental changes brought about by natural or human activities result in either scouring of river bed or erosion of river banks. This subsequently affects the river geomorphology with the overall result of hampering marine transportation, have a devastating effect on the environment, adjoining facilities and marine structures. These changes in river flow as a result of sediment-water interaction cannot be effectively managed without the full knowledge and understanding of river hydrodynamics and sediment transport mechanism [1]. In the presence of waves and current, the current boundary layer fills the whole flow depth while the wave boundary layer remains small [2]. Current is usually the main transporter of the sediments stirred up by the waves.

Bank erosion is a key process in river morphodynamics which affects the channel mobility, flood plain evolution and associated habitat development [3]. This causes damage to riparian lands and infrastructure [4] and mobilizing sediments that can cause turbidity, nutrient and contaminant problems [5,6]. Many factors influence scouring rates but the most important driving factors include the fluid flow, the amount of turbulence and presence of waves.

Generally, erosion occurs on the outer (concave) bank of the meander bend and accretion occurs on the inner (convex) bank of the meander bend. Bank erosion occurs through two dominant processes: hydraulic action and mass failure [7]. The larger the water velocity, the greater the energy of the flow and the greater the potential for hydraulic action to detach material from the bank. Mass failure occurs when a large slab of material shears away from the bank and slides or slumps to a lower position. The tendency of a river bank to mass failure however, depends on the geometry, structure and material properties of the affected bank [8]. When the bank toe has been eroded and the bank height and angle are changed to a point where the gravitational forces are larger than the forces holding the bank together, failure occurs [9].

Though the Navier-Stokes and continuity equations represent a generally accepted mathematical description of fluid flow, there is no comparable model for the complete interaction of flow, sediment transport and bed evolution [10]. The aim of this study was to model the velocity distribution at inner, centerline and outer bend of the selected stretch of Nun River at upstream midstream and downstream. Field observation confirmed bank erosion at inner bend and sediment deposition at outer bend. The scope of this study was limited to the application of computational methodology to predict the interaction between river bathymetric shape, flow currents and associated appurtenances arising from the study stretch of the river.

2. MATERIALS AND METHODS

2.1 Study Area

Nun River which is located in southern Nigeria is a direct continuation of River Niger.

Nun River lies on Latitude: 4°17' 12" N and Longitude 6°04' 20" E.

River Niger bifurcates into the Nun and Forcados rivers about 20 miles (32 km) downstream from Aboh. The Nun river flows through sparsely settled zones of freshwater and mangrove swamps and coastal sand ridges before completing its 100-mile (160-km) south westerly course (see Fig. 1) to the Gulf of Guinea, a wide inlet of the Atlantic Ocean, at Akassa.

2.2 Traverse Survey

Traverse survey was carried out in order to establish the geometry of the river. The survey was carried out on existing survey points to provide controls along the study area of the river. These controls were used to detail any existing features within the area surveyed.

2.3 Bathymetric Survey

The source of bathymetric data is the Shell Petroleum Development Company Geomatics department. Bathymetric survey was to establish the riverbed geometry. This was carried out using multi-beam echo sounder. All elevations were expressed in metres. The depth was subsequently reduced to the required datum, in line with the coordinate system of the locality (Lagos Datum) as shown in Fig. 2.



Fig. 1. Niger Delta area map showing Nun river [11]

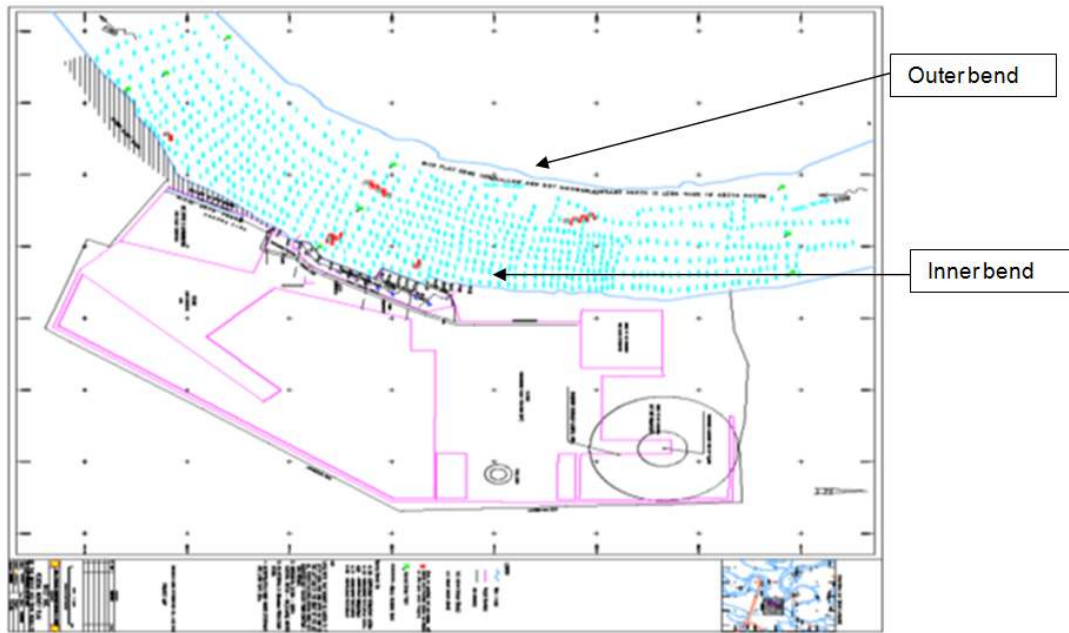


Fig. 2. Bathymetric map of a stretch of Nun River [12]

2.4 Water Current Measurements

A current recording meter (Aandreaa RCM 9) with acoustic Doppler current sensor 3620 was used in water current measurements. During operation, the current meter was mounted on a

mooring frame and positioned at a location for the measurement. This was done in the upstream, midstream and downstream areas of the river stretch within the study area. The average data from the water current measurements are as presented in Table 1.

Table 1. Water velocity measurement

Date	Location	Surface			Middle			Bottom					
		Time (hr)	velocity (m/sec)		Direction (deg)	Time (hr)	velocity (m/sec)		Time (hr)	velocity (m/sec)			
			Min	Max			Min	Max		Min	Max		
6/11/2015	Up stream	9		0.95	350	9.1		1.85	350	9.5		0.2	350
		14.3	0.65		260	15.4	1.1		188	13.5	0		250
8/11/2015	Mid-stream	12		0.5	345	12.1		0.75	340	12.2		0.1	350
		13.3	0.25		285	13.4	0.4		280	13.5	0.1		290
9/11/2015	Down stream	8		0.4	290	8.1		0.5	290	8.2		0	290
		9.3	0.1		45	9.1	0.1		260	9.2	0.1		200

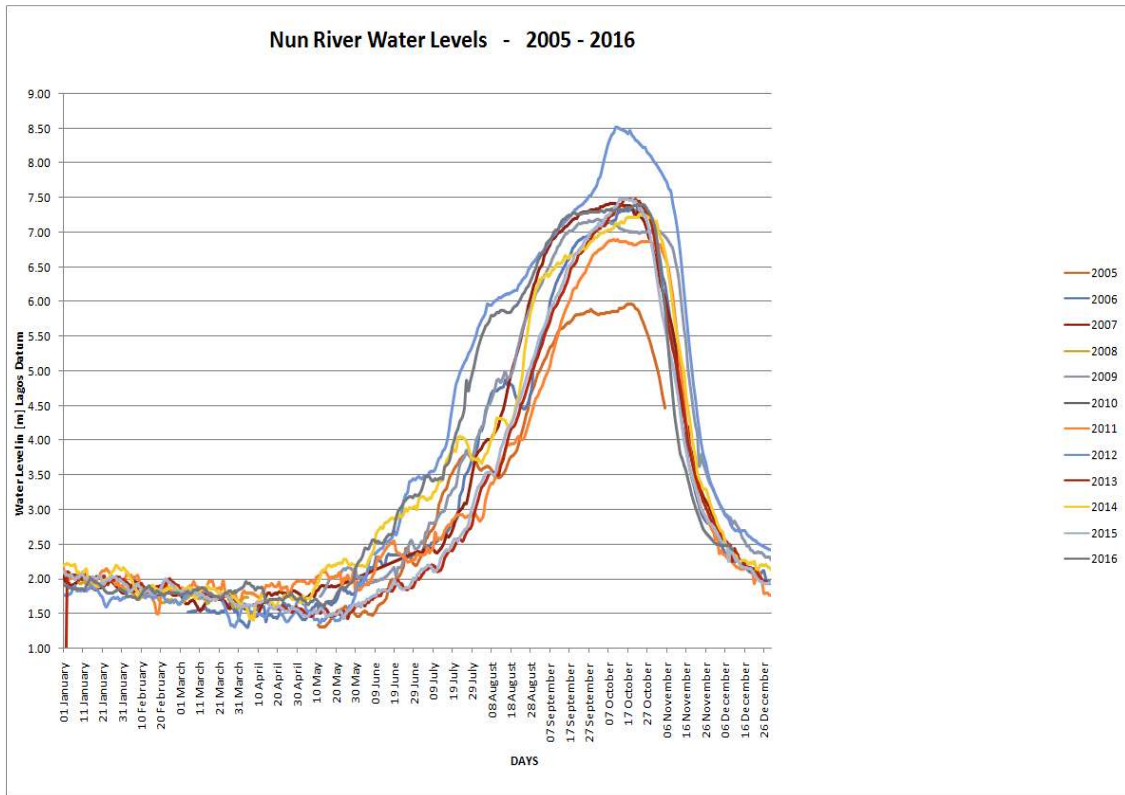


Fig. 3. Nun River water levels for 11-year period (2005 – 2016) [13]

2.5 Hydrographic Survey

Flood gauge was installed to the Jetty area to measure the water surface elevations and the time of observation noted. The gauge was a 10m staff, painted and marked in a manner to cover the lowest and highest known depths of the water within the study area. Readings were taken at intervals of one day. The results of the flood gauge of previous years between 2005 and 2016 are as shown in Fig. 3 above.

3. MODEL CONSTRUCTION

3.1 Mesh Construction

The river geometry was constructed using a series of 1:1000 maps. The river reach considered stretches to 2,000 m length and width varying between 350 m to 400 m. In the horizontal plane, the domain was covered with a near rectangular mesh with cross sections taken at every 20 m in both x and y directions and 1 m in z-direction; with h and k units denoting x and y directions while θ unit denotes the z direction.

The main channel depth varies from 0 to 13 metres, with mesh prepared at 0, -5, and -10 m (beneath the surface), respectively. A total of 2,445 nodes were generated to give equal numbers of governing simultaneous linear equations (see Fig. 4).

3.2 Governing Equation

3.2.1 Equations of flow

The governing equations for the hydrodynamics are assumed same as Navier- Stokes equations with the inclusion of lateral inflow term [14] and are given as Equations (1 – 4):

$$\frac{\partial u}{\partial x} + \frac{\partial v}{\partial y} + \frac{\partial w}{\partial z} = 0 \quad (1)$$

$$\frac{\partial u}{\partial t} + \frac{u\partial u}{\partial x} + \frac{w\partial u}{\partial z} = \frac{-1}{\rho} \frac{\partial p}{\partial x} + \frac{\partial}{\partial x} \left(Ux \frac{\partial u}{\partial x} \right) + \frac{\partial}{\partial z} \left(Uz \frac{\partial u}{\partial z} \right) + q_{lx} \quad (2)$$

$$\frac{\partial v}{\partial t} + \frac{u\partial v}{\partial x} + v \frac{\partial v}{\partial y} + \frac{w\partial v}{\partial z} = \frac{1}{\rho} \frac{\partial p}{\partial y} + \frac{\partial}{\partial x} \left(Ux \frac{\partial v}{\partial x} \right) + \frac{\partial}{\partial y} \left(Uy \frac{\partial v}{\partial y} \right) + \frac{\partial}{\partial z} \left(Uz \frac{\partial v}{\partial z} \right) + q_{ly} \quad (3)$$

$$\frac{\partial \rho}{\partial t} + P_g = 0 \quad (4)$$

Where: t = time, x, y, z = Cartesian coordinates; u, v, w = Velocity components in the x, y and z directions, respectively; q_{lx} , q_{ly} = lateral inflows from the banks due to flood inundation.

3.2.2 Boundary conditions

The following boundary conditions are applicable:

- i) Velocity is assumed 0 at the water surface, river bed and coastal lines;
- ii) Velocity component perpendicular to the coastline is zero;
- iii) Inlet and outlet boundary conditions were provided through field measurements; and
- iv) Current velocity due to lateral inflow was measured at the inflow points in the field.

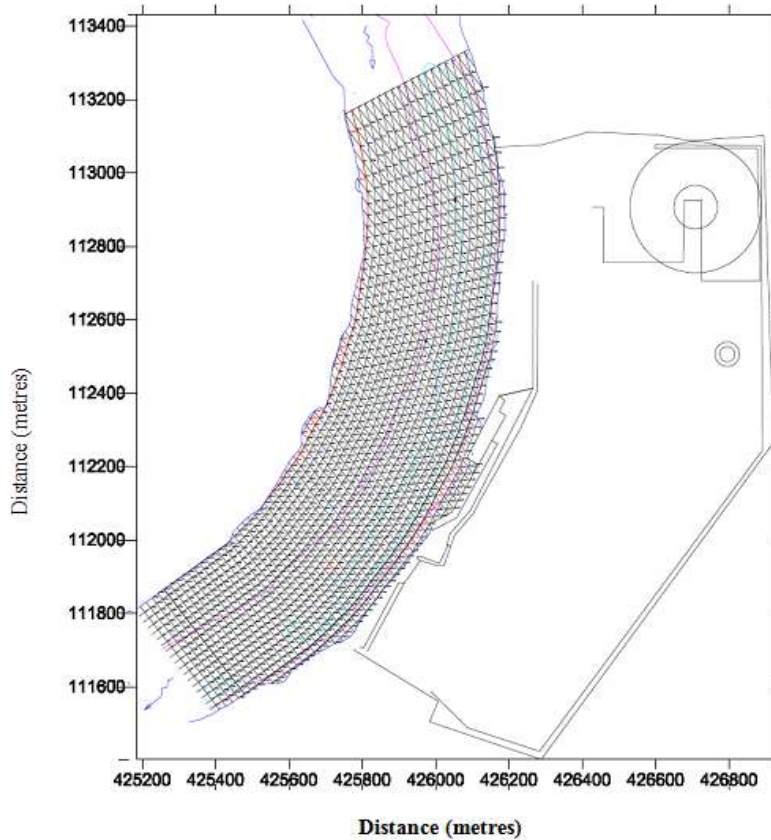


Fig. 4. Surface layer mesh (Reference datum: 0.0m low water level)

3.3 Application of Finite Difference Method

The model applied an implicit (Crank Nicholson's procedure) in solving the governing differential equations in three dimensions. In the finite difference method, a typical solution grid which is a network of equally spaced orthogonal lines with computational nodes at the intersections or in the centre of each square is formed [15]. In finite difference model, the boundaries of channels and other water bodies are approximated by stair-step edges following the grid.

The Equation Solver (EKU 2.8) is a 3-dimensional hydrodynamics sediment concentration and velocity prediction model using finite difference approach. It was coupled using conservation of mass and momentum for the hydrodynamics (Navier-Stokes equations) with the inclusion of

lateral inflow as modified by Dike and Agunwamba [14].

The Eku 2.8 discretizes along boundaries and contours, and then uses transform relations to map the discretization to a rectangular grid for solution. The basic equations are modified to represent currents and tides in the transformed system. The current study uses conservative finite difference method for discretization. Conservative finite difference method has the same conservation properties as finite volume method. As the current study utilizes structured grids, the finite difference method is simple and effective. It is also very easy to obtain higher order schemes on regular grids. It is very stable [16].

By applying Crank –Nicholson implicit method [17] at points in time halfway between two nodes and substituting the finite difference implicit approximations (first order derivatives) into Equation (2), we have:

$$\begin{aligned} & \left[-1 + \frac{\mu_x}{h^2} + \frac{\mu_y}{k^2} + \frac{\mu_z}{l^2} \right]^{i,j,k,\theta} + \left[\frac{u}{4h} + \frac{c_D u}{8h} - \frac{\mu_x}{2h^2} \right]^{i+1,j,k,\theta} + \left[-\frac{u}{4h} + \frac{c_D u}{8h} - \frac{\mu_x}{2h^2} \right]^{i-1,j,k,\theta} \\ & + \left[\frac{v}{4k} - \frac{\mu_y}{2k^2} \right]^{i,j+1,k,\theta} + \left[-\frac{v}{4k} - \frac{\mu_y}{2k^2} \right]^{i,j-1,k,\theta} + \left[\frac{w}{4l} - \frac{\mu_z}{2l^2} \right]^{i,j,k+1,\theta} + \left[-\frac{w}{4l} - \frac{\mu_z}{2l^2} \right]^{i,j,k-1,\theta} \\ & = \left[\frac{(u_x - u_l)n}{wD} \right] f_x \end{aligned} \tag{5}$$

Equation (5) is simplified to give the following sets of simultaneous linear equations with the inclusion of boundary conditions where i, j, k, θ stand for the nodal points (see Equation 6). The same procedure was applied to Equations (3) and (4) to reduce them to a system of simultaneous equations.

$$\begin{aligned} & [0.005] * \{i, j, k, \theta\} + [0.01] * \{i+1, j, k, \theta\} - [0.01] * \{i-1, j, k, \theta\} \\ & + [0.01] * \{i, j+1, k, \theta\} - [0.01] * \{i, j-1, k, \theta\} \\ & - [0.3] * \{i, j, k+1, \theta\} + [0.3] * \{i, j, k-1, \theta\} \\ & = \left[\frac{(u_x - u_l)_{ave} n}{wD} \right] f_x \end{aligned} \tag{6}$$

But $\mu_x = \mu_y = \mu_z = 0.001 \text{ mg} \cdot \text{m}^{-1} \cdot \text{s}^{-1}$ (assumed)

$U_{ave} = 0.25 \text{ m/s}$ average velocity in x direction

$V_{ave} = 0.375 \text{ m/s}$average velocity in y direction (results of Current Measurements).

By integrating Equation (1) and substituting values of u_{ave} and v_{ave} , into it, we obtain $w_{ave} = 0.625 \text{ m/s}$.

Also, given that $h = 20 \text{ m}$, $k = 20 \text{ m}$, and $l = 1 \text{ m}$,

$C_d = 0.2$ (for turbulent flows) [18].

Substituting values of $U, V, W, h, k, l, C_d, U_i, w, D, H, n$ and f into Equation (6),

we obtain the values of coefficients at different nodes in 3-Dimensions.

This is used in generating the values of velocities in x, y and z directions at different nodes and at $T = T_0$, where i, j, k, θ stand for the nodal points.

3.4 Model Input Data and Solution

The following actions are necessary to run Eku 2.8:

- i) The initial or assumed values of $u, v, w, h, k, l, C_d, U_i, w, D, H, n, Ws, C,$ and f were inputted into the Eku 2.8 platform to generate the values of the coefficients at different nodes in 3-dimensions.
- ii) The generated coefficients at each node were automatically coupled into the mesh by the software with the inclusion of the initial boundary conditions to generate the sets of simultaneous linear equations as in the solution table.
- iii) The equations numbering about 2,445 were subsequently solved to generate the

values of current velocity at different nodal points in three dimensions.

4. RESULTS AND DISCUSSION

4.1 Results

The velocity distributions at the nodes were simulated by solving the governing Navier Stokes equations of flow implicitly using Crank Nicolson procedure in three dimensions. On the velocity distribution two sets of plots were made. First, the longitudinal velocity profile stretching from upstream, midstream to downstream was examined for four cases. Cases 1 – 4 examine the distribution at 20, 40, 60, and 80 metres away from both the inner and outer bends (see Figs. 5 – 8). Second, the traverse velocity distributions were plotted for upstream, midstream, and downstream sections (see Fig. 9).

The predicted velocity against observed values were regressed using XLSTAT 2016 and the results are presented in Table 3 (goodness of fit, R^2 of 0.927), Table 4 for analysis of variance (output), and Fig. 10 confirming a good linear relationship between observe and a predicted value.

4.2 Discussion

The longitudinal velocity profile at the inner and outer bends, 20m offset away from the bank, (see Fig. 5) showed a positive velocity profile at the upstream section of the river up to 600m stretch before it became negative. The negative velocity progressed up to 640 m stretch before it became positive again to the end of 2,000 m stretch. The outer bend on the other hand demonstrated a gradual positive velocity which also became negative between 120 m and 600 m stretch and thereafter became positive for 2,000 m stretch.

Table 2. Measured and predicted velocity distributions of Nun River

Location	Measured and predicted longitudinal velocities					
	Surface layer (0 m)		Mid-depth (-5 m)		Bottom depth (-10 m)	
	Measured average	Predicted average	Measured average	Predicted average	Measured average	Predicted average
Left bank (Up stream)	0.8	0.845	1.475	1.542	0.105	0.00134
Right bank -Jetty (Mid stream)	0.375	0.3218	0.575	0.6621	0.1	0
Centre (Downstream)	0.25	0.3357	0.3	0.641	0.095	0

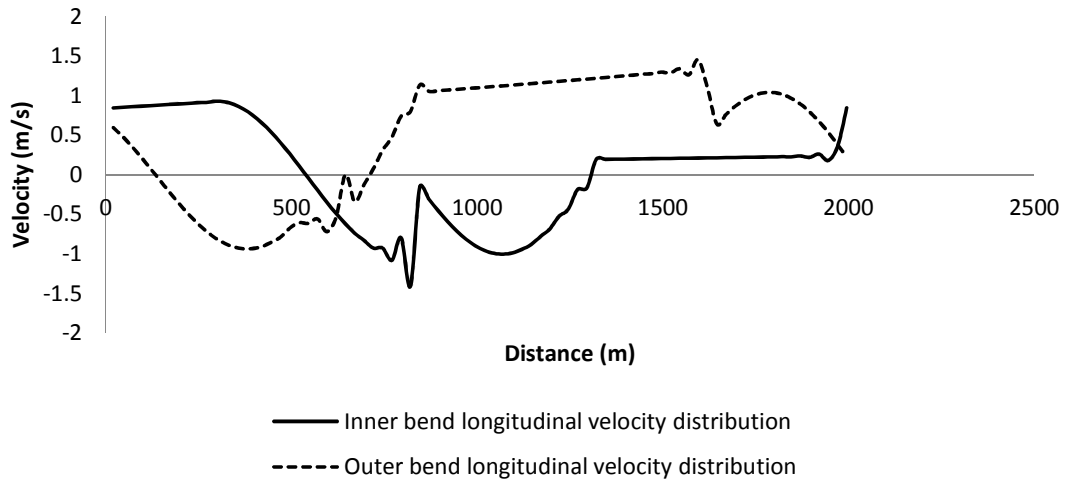


Fig. 5. Longitudinal velocity distribution at inner and outer bends 20 m away from banks

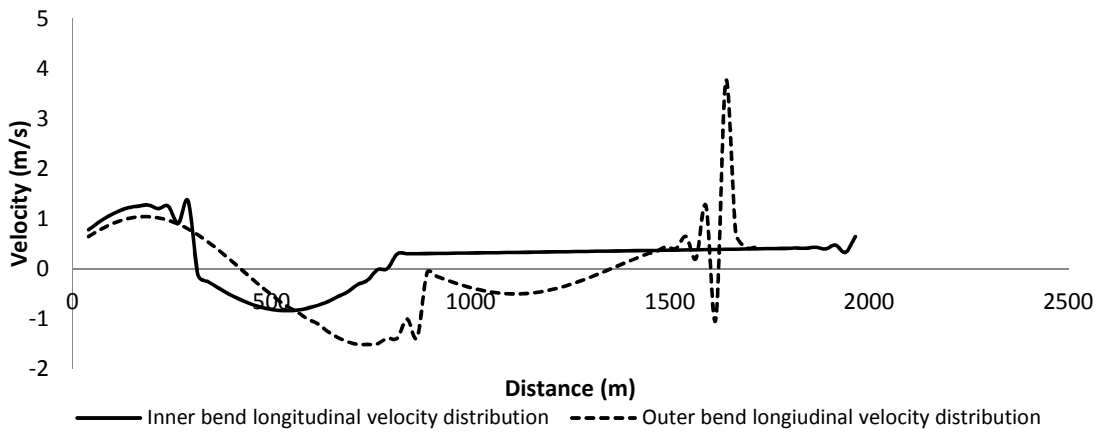


Fig. 6. Longitudinal velocity distribution at inner and outer bends 40 m away from banks

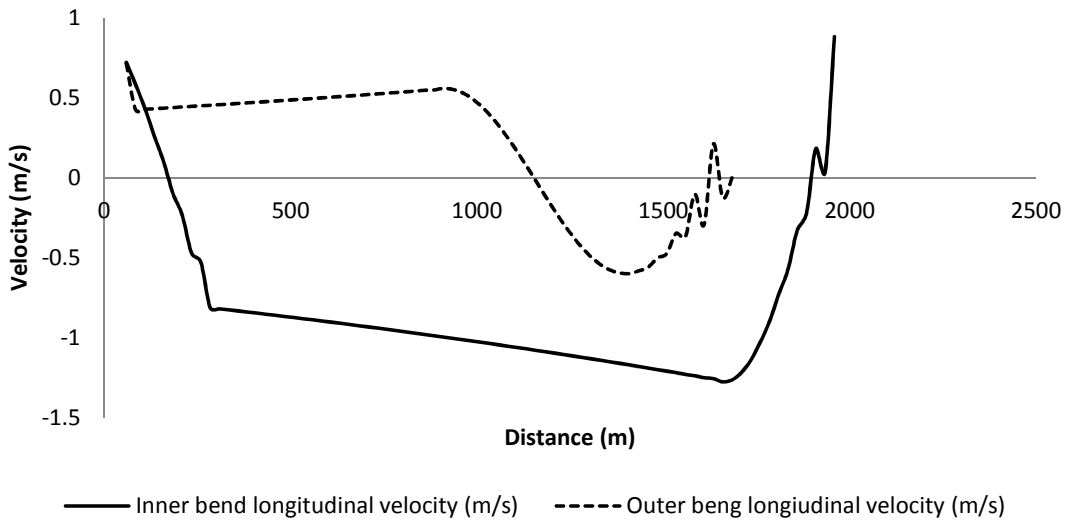


Fig. 7. Longitudinal velocity distribution at inner and outer bends 60 m away from banks

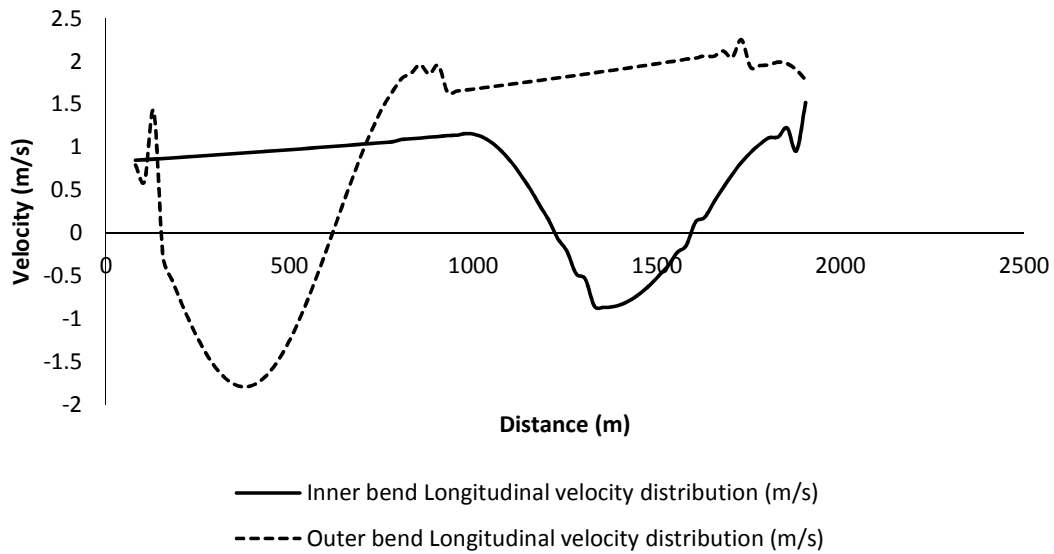


Fig. 8. Longitudinal velocity distributions at inner and outer bends 80 m away from banks

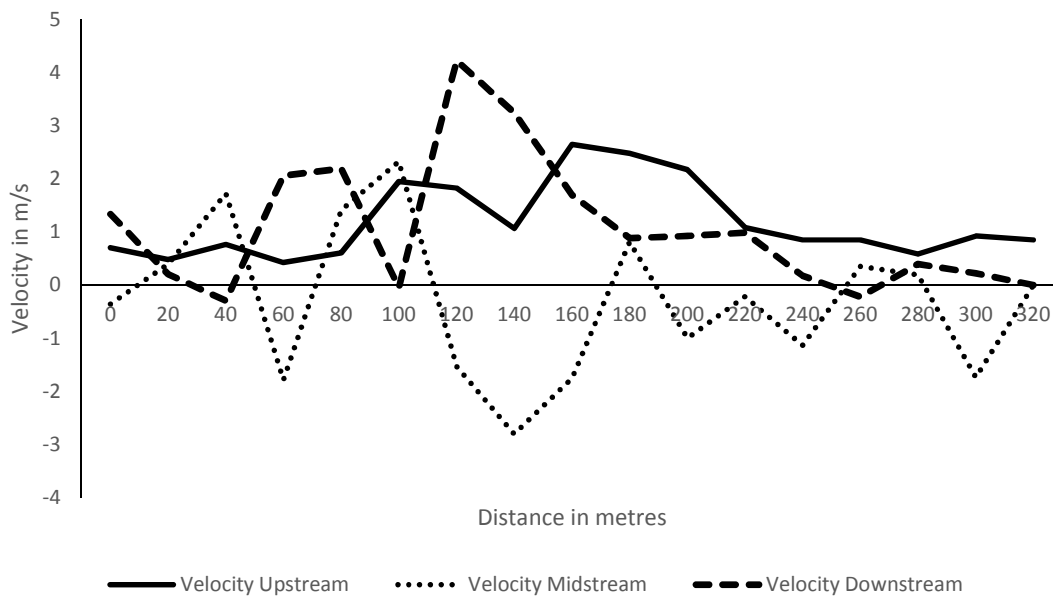


Fig. 9. Traverse Velocity Profile of Upstream, Midstream and Downstream

The longitudinal velocity distribution at 40m offset from the bank as in Fig. 6 showed positive velocity profiles for both inner and outer bends up to 300 m stretch for inner bend and 400 m stretch for outer bend. While the inner bend exhibited positive velocity profile from the 800 m offset to 2000 m length, the outer bend continued the negative velocity trend to the 1420 m stretch from the offset.

As we move further away from the bank by 60m (Fig. 7), the outer bend showed a remarkable positive velocity profile from the offset point to 1200 m stretch before becoming negative. It was negative for a short distance, 1200 m to 1550 m stretch and thereafter, it became positive again.

The inner bend however showed a negative velocity profile from the 60 m offset throughout the entire stretch. At the 80 m offset from the

bank (Fig. 8), the inner bend showed a positive velocity profile up to 1250m stretch, a negative profile between 1250 and 1540 stretch. It was positive to the end of the 2000m stretch. For the outer bend, the velocity profile moved from positive at 80 m offset to negative at 100m offset through 600 m, thereafter, it was positive throughout the stretch.

Table 3. Goodness of fit statistics (y)

Observations	9.000
Sum of weights	9.000
DF	7.000
R ²	0.927
Adjusted R ²	0.916
MSE	0.017
RMSE	0.130
MAPE	37.932
DW	1.737
Cp	2.000
AIC	-34.921
SBC	-34.526
PC	0.115

Lateral (transverse) velocity profiles were also taken at upstream, mid-stream and downstream locations of the 2,000 m stretch and examined. Whereas the upstream section showed an all positive velocity profile across the 320 m stretch

from the bank, the velocity profile at mid-stream showed a combination of positive and negative profiles while the downstream exhibited a near-all positive profile. However, they all displayed a remarkable jump at the centerline areas between the 100 and 180m stretch across the width.

From the forgoing analysis, flow on the surface layer appears relatively lamina due to smooth and near uniform bathymetric shape at the surface river bank level, the velocity appears unsteady with a lot of eddies especially at the mid and bottom layers. The results indicate that current velocity decreases gradually from upstream boundary of the river and gradually increases downstream (see Figs. 5-7) Along the river banks, especially at the outer bends, the current become high and circulatory, probably due to the river curvature and impediments to flow caused by the irregular bank profiles and river on-going training works [1]. At the inner bend, significant bank erosion was not noticeable (during physical assessment) probably due to the irregular bathymetric shape of the river and reduced current velocity which resulted in siltation instead of scouring. At the up- and down-stream sections of the outer bend, the landing jetty position (see Fig. 3) altered the river flow patterns within this stretch, which resulted in agitated flow and turbulent effects as shown in Figs. 5 to 9.

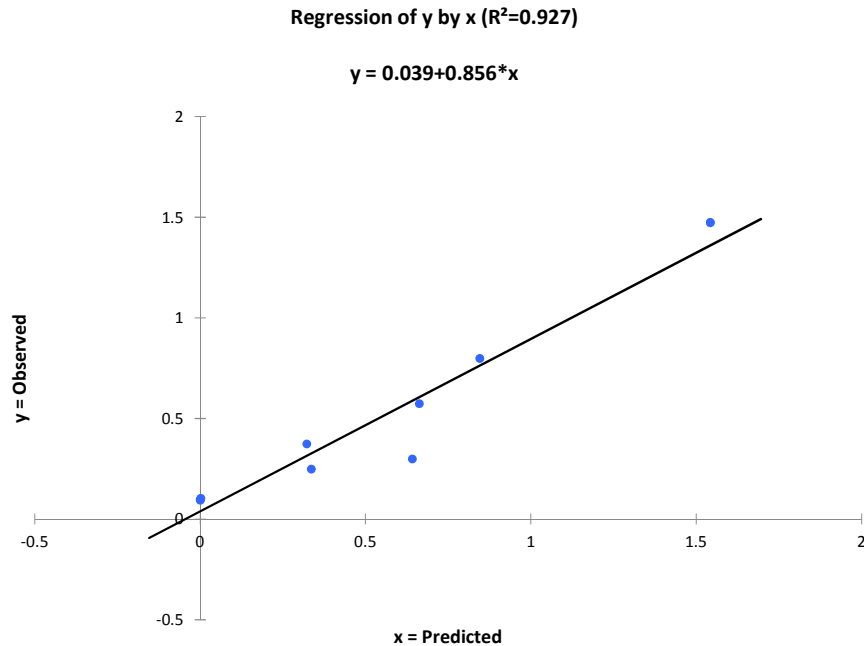


Fig. 10. Plot of regression of observed against predicted data sets

Table 4. Analysis of variance

Source	DF	Sum of squares	Mean squares	F	Pr > F
Model	1	1.505	1.505	88.422	< 0.0001
Error	7	0.119	0.017		
Corrected Total	8	1.624			

Average predicted velocities of 0.85 m/s, 1.542 m/s and 0m/s compared favorably with 0.8m/s, 1.475 m/s and 0.09 m/s obtained from field measurement for upstream, midstream and downstream boundaries. At the bed and bank boundaries, zero velocities were assumed, while at the inlet and outlet boundaries, the field current measurements were used as earlier stated in the boundary conditions. The model proved very useful in predicting the velocity distribution of Nun River; higher versus lower velocities at inner and outer bends, with resultant effect of erosion and sediment deposition accordingly. The result of this study may be considered an important contribution to the improvement of sediment and erosion risk management.

5. CONCLUSION

Based on the results of this study, the following conclusion can be drawn:

- i). Field data were inputted into the numerical model, EKV2.8 to simulate Nun river's flow velocity distributions. Average predicted velocities of 0.85 m/s, 1.542 m/s and 0 m/s which compared favourably with 0.8m/s, 1.475 m/s and 0.09 m/s obtained from field measurements for upstream, mid-stream and downstream locations, respectively.
- ii). The predicted results have approximate goodness of fit, R^2 of 0.92 for velocity distribution using Pearson product-moment method.
- iii). The model proved very useful in predicting velocity distributions for better insight on bank erosion at Nun River, higher and lower velocities at the inner and outer bends that confirmed evidence of erosion and deposition of sediments, respectively.

6. RECOMMENDATION

The following recommendation is made:

The result of this study can be considered an important contribution to the improvement of erosion risk management and will contribute to

comparative studies on erosion and current management of the river.

COMPETING INTERESTS

Authors have declared that no competing interests exist.

REFERENCES

1. Dike CC, Nwaogazie IL, Uba LC. Prediction of eddy current and scour hole positions along river beds. PENCIL Publication of Physical Sciences and Engineering. 2015;1:1-10.
2. Mohammad SA. 3D numerical modeling of sediment transport under current and waves, Norwegian University of Science & Technology. Department of Civil and Transport engineering. June; 2013.
3. Goodson JM, Gurnell AM, Angold PG, Morrissey IP. Riparian seed banks along the lower River Dove, UK, Geomorphology. 2002;47:45-60. DOI: 10.1016/S0169-555X(02)00140-X
4. Simon A. Adjustment and recovery of unstable alluvial channels, identification and approaches for engineering management. Earth Surf. Processes Landforms. 1995;20:611-628. DOI: 10.1002/esp.3290200705
5. Bull IJ. Magnitude and variation in the contribution of bank erosion to the suspended sediment load of the River Severn, UK, Earth Surf. Processes Landforms. 1997;22:1109-112. DOI: 10.1002/(SICI)1096-9837(199712)22:12
6. Reneau SL, Drakos PG, Katzman D, Malmon DV, McDonald EV, Rytz RT. Geomorphic controls on contaminants distribution along an ephemeral stream. Earth Surf. Processes Landforms. 2004;29:1209-1223. DOI: 10.1002/esp.1085
7. Posner A, Duan J. simulating River meandering processes using stochastic bank erosion coefficient. Geomorphology. 2012;163&164:26-36.

8. Knighton D. Fluid forms and processes: A new perspective. London: Holder Education; 1998. ISBN:9780340663134
9. Simon A, Pollen-Bankhead N, Mahacek V, Langendoen E. Quantifying reduction of mass failure frequency and sediment loadings from stream banks using toe protection and other means. Lake Tahoe. United States. Journal of the American Water Resources Association. 2009;45(1): 170-178.
10. Spasojevic M, Holly FM. Two and three dimensional numerical simulation of mobile-bed hydrodynamics and sedimentation. Sedimentation engineering processes, measurements, modeling, and practice. Marcelo HG, ed., American Society of Civil Engineers. 2008;683-761.
11. Google Maps. Imagery @2016 Digital Globe, CNES/Astrium. Available:<https://www.google.com.ng/maps>
12. Shell Petroleum Development Company, SPDC. The shell petroleum development company of Nigeria limited. Koroama Shoreline Protection Design (Report on Koroama Manifold/Taylor Creek Study); 2012.
13. Shell Petroleum Development Company, SPDC. The shell petroleum development company of Nigeria limited. Koroama Shoreline Protection Design (Report on Koroama Manifold/Taylor Creek Study); 2016.
14. Dike CC, Agunwamba JC. Modelling of sediments concentration distribution and siltation prediction in the dredged canals of the Niger Delta estuarine region, Nigeria. Research Gate; 2010.
15. Nwaogazie IL. Finite element modelling of engineering systems. Published by University of Port Harcourt Press. Port Harcourt, Nigeria; 2008.
16. Hassan SM. Hydrodynamic and sediment transport modeling of deltaic sediment processes. Department of Civil and Environmental Engineering. Louisiana State University; 2003.
17. Kiely G. Environmental Engineering. McGraw-HILL International (UK) Limited Publications; 1998. ISBN0-07-116424-3 (International Edition)
18. Rajput RK. Fluid mechanics and hydraulic machine (Third edition). S. Chand & Company Ltd. Ram Nagar. New Delhi-110055; 2007. ISBN 81-219-1666-6

© 2017 Nwoko et al.; This is an Open Access article distributed under the terms of the Creative Commons Attribution License (<http://creativecommons.org/licenses/by/4.0>), which permits unrestricted use, distribution, and reproduction in any medium, provided the original work is properly cited.

Peer-review history:

*The peer review history for this paper can be accessed here:
<http://sciencedomain.org/review-history/18966>*